Acta Physiologica Sinica, June 25, 2006, 58 (3): 244-254
http://www.actaps.com.cn

Research Paper

Cigarette smoke extract inhibits the proliferation of alveolar epithelial cells and induces apoptosis

JIAO Zong-Xian, AO Qi-Lin*, XIONG Mi

Department of Pathology, Tongji Medical College, Huazhong University of Science and Technology, Wuhan 430030, China

Abstract: Cigarette smoke extract (CSE) contains abundant oxidants and free radicals. Oxidative stress caused by cigarette smoking results in the destruction of the alveolar cell walls and emphysema. However, there exists discrepancy about how CSE works in the process. In the present study, we observed the effect of CSE on the cell growth of type II alveolar epithelial cell-derived A549 cell line, and provided molecular understanding of this effect. The MTT assay results showed that CSE decreased the cell viability of A549 cells in a dose- and time-dependent manner, and cell cycle was arrested in G_1/S phase. Furthermore, CSE-induced apoptosis of A549 cells was verified by Hoechst 33258 staining, electron microscopy in morphology, and the appearance of DNA fragmentation and annexin V-FITC/propidium iodide (PI) staining assay at molecular level. It was found that CSE treatment resulted in the upregulation of Fas/APO-1 receptor and activation of caspase-3. CSE also initiated accumulation of intracellular reactive oxygen species, which was detected by laser confocal microscopy. Taken together, CSE could inhibit the cell growth and induce apoptosis of A549 cells through Fas receptor pathway. Oxidative stress caused by CSE may be the radical factor leading to apoptosis as well as cell growth inhibition in alveolar epithelial cells.

Key words: cigarette smoke; alveolar epithelial cells; apoptosis; Fas receptor

香烟烟雾提取物抑制肺泡上皮细胞的增殖并诱导其凋亡

焦宗宪，敖启林*，熊 密

华中科技大学同济医学院病理学系， 武汉 430030

摘 要： 香烟烟雾提取物(cigarette smoke extract, CSE)中含有丰富的氧化剂和自由基，由它所引起的氧化应激可导致肺泡壁的损伤进而发展为肺气肿。近年来，围绕CSE 损伤肺泡壁作用机制的研究较为活跃，但其结果却一直存在着分歧。本实验的目的是观察CSE 对肺泡II 型上皮细胞的损伤作用并探讨与其相关的分子机制。MTT 比色法的结果显示，CSE 以时间和剂量依赖性的方式降低细胞的增殖活力，流式细胞术的分析结果表明细胞增殖周期被阻滞在G_1/S 期。Hoechst 33258 染色以及透射电镜观察从形态上确认CSE 诱导细胞凋亡的发生，DNA 梯的出现和Annexin V-FITC/ 碘化丙啶双染色的结果从分子水平得到进一步的证实。同时，运用流式细胞术检测到CSE 诱导的凋亡伴随着Fas 受体的高表达和caspase-3 的显著活化。另外， 使用H_2DCFDA 染色，经激光共聚焦显微镜术测得细胞内氧自由基在细胞受到CSE 刺激以后大量快速积累。结果表明CSE 能够抑制肺泡II 型上皮细胞来源的A549 细胞的生长和增殖，并诱导细胞凋亡，由Fas 受体所介导的死亡受体途径参与此凋亡过程，而CSE 所引起的氧化应激则可能是阻止肺泡上皮细胞生长增殖并诱导其凋亡的始动因素。

关键词： 香烟烟雾；肺泡上皮细胞；凋亡；Fas 受体
中图分类号： Q471; R363.2+1

Cigarette smoke contains about 1×10^{17} oxidants/free radicals and 4 700 chemical compounds, including aldehydes and quinones per puff, and many of these are relatively long-lived such as tar-semiquinone that can generate hydroxyl radicals (·OH) and hydrogen peroxide (H_2O_2) by the Fenton reaction[1]. Cigarette smoking is the major etiological factor in the pathogenesis of chronic obstructive pulmonary disease (COPD)[2], and oxidative stress caused

Received 2006-03-13 Accepted 2006-04-09

*Corresponding author. Tel: +86-27-83662556; E-mail: aoqilin@263.net

by cigarette smoking is thought to induce a chronic inflammatory response in the lungs which results in the destruction of the alveolar cell walls and emphysema.

Emphysema is characterized by enlargement of distal airspaces due to destruction of alveolar wall endothelial cells, epithelial cells, and connective tissue resulting from both protease/antiprotease and oxidant/antioxidant imbalances[3,4]. Among the various cell types which compose the lung, the epithelial cells of the alveolar structure appear to be the major target for oxidant injury[5-8]. These epithelial cells are of two types: type I and type II cells. It is now well established that type II cells are the stem cells of the alveolar epithelium, and that repair of damaged alveolar surface is dependent on their ability to replicate and to provide additional cells that have the potential to undergo transition into type I cells. After oxidant injury, the rapidity of initiation of type II cell proliferation is crucial for a proper healing. Therefore, characterization of the mechanisms involved in the block of type II cell replication by oxidants appears to be critical for the understanding of many lung diseases associated with oxidative stress. However the mechanisms through which type II cell replication is regulated upon oxidant exposure remain poorly understood.

Recently, it has been proposed that apoptosis of alveolar wall cells occurs in response to cigarette smoking, resulting in progressive cell loss and emphysema[5-9]. However, contradiction arises in terms of how cigarette smoking affects this process, because both stimulatory and inhibitory potentials of smoking on apoptosis have been demonstrated. Wickenden *et al*.[10] offered that cigarette smoke extract (CSE) could induce necrosis of alveolar epithelial cells instead of apoptosis through inhibition of caspase activation, while Besnard *et al*.[11] reported hyperoxia-induced apoptosis through the Fas pathway in type II alveolar cell-derived cell line. Therefore it is quite necessary to discover the mechanisms through which CSE affects alveolar epithelial cells.

In order to solve the argument, one of the aims of the present study was to clarify whether CSE could indeed induce apoptosis of human type II alveolar epithelial cells. Since Fine *et al*.[12] postulated that Fas-dependent apoptosis may be involved in the regulation of alveolar epithelium injury and may represent an important mechanism of repair processes, another purpose of the study was to investigate the possible response of Fas expression in CSE-induced human alveolar epithelial cells for the first time. A549 cells, a type II alveolar epithelial cell line, were chosen as surrogate cells to represent type II alveolar epithelial cells.

1 MATERIALS AND METHODS

1.1 *Chemicals and reagents*

Fetal bovine serum (FBS; Sijiqing, Hangzhou, China), Dulbecco's modified Eagle's medium (DMEM; Hyclone, Logan, UT), Monoclonal antibody to human CD95 (Fas/APO-1)-FITC (Caltag Laboratories, Burlingame, CA). Cigarettes of a domestic brand were purchased from Lanzhou Tobacco (Lanzhou, China). 3-(4,5-dimethylthiazal-z-yl)-2,5-diphenylterazolium (MTT), chromatin dye bisbenzimide (Hoechst 33258), propidium iodide (PI), and 2',7'-dichlorodihydrofluorescein diacetate (H_2DCFDA) were obtained from Sigma Chemical Company (St. Louis, MO, USA). The annexin V fluorescein isothiocyanate (FITC) apoptosis detection kit and CaspGLOW™ fluorescein active caspase-3 staining kit were purchased from BioVision (Mountain view, CA, USA). All chemicals were of analytical reagent grade.

1.2 *Preparation of CSE*

CSE was prepared by a modification of the method of Harvey and Aaron[13]. In brief, two cigarettes without filters were combusted with a modified syringe-driven apparatus. The smoke was bubbled through 50 ml of serum-free DMEM, and the resulting suspension was adjusted to pH 7.4 and then filtered through a 0.22 μm pore filter to remove bacteria and large particles. The resulting CSE was applied to epithelial cell cultures within 30 min of preparation.

1.3 *Cell culture*

The human type II alveolar epithelial cell line A549 was obtained from the Cell Bank of Chinese Academy of Sciences (Shanghai, China). A549 cells were grown in DMEM supplemented with 10% FBS, 100 U/ml penicillin, 100 μg/ml streptomycin and 2 mmol/L *L*-glutamine in a humidified incubator with 5% CO_2 at 37 °C. The culture medium was renewed every 2 to 3 d.

1.4 *Analysis of cell viability*

Cell viability was determined by MTT assay[14]. Cells were seeded in 96-well plates at 1×10^4 cells per well and cultured in DMEM containing 10% FBS until the cells attached. The medium was then changed to serum-free for 16 h until the cells had grown to 70%~80% confluence. The cells were then treated with culture medium and different concentrations of CSE, i.e., 5%, 10%, or 20% CSE for 24 h, 48 h and 72 h in serum-free medium. After the cells were incubated with MTT for another 4 h at 37 °C, the medium was removed and dye crystal formazan were solubilized in 150 μl dimethyl sulphoxide (DMSO). Absor-

bance was measured at 570 nm by use of a Bio-Tek Powerwave X microplate reader (BioTek Instruments, Inc., USA).

1.5 *Cell cycle analysis*

Cells were seeded in 75 ml culture flasks at 5×10^5 respectively and cultured in DMEM containing 10% FBS until the cells attached. The following treatment was the same as described above. Cell cycle stage was analyzed by flow cytometry[15]. Aliquots of 1×10^6 cells were harvested by centrifugation, washed in PBS, fixed with ice-cold 70% ethanol for at least 24 h and then treated with 20 mg/L RNase for 30 min. PI was added to a final concentration of 20 mg/L. DNA contents of the samples were analyzed on a Coulter Epics XL flow cytometry (Beckman-Coulter Inc., Fullerton, CA, USA), and the number of cells in every phase was calculated using Multicycle software (Phoenix Flow System, San Diego, CA, USA).

1.6 *Detection of apoptosis*

1.6.1 *Hoechst 33258 staining*

A549 cells were grown on glass coverslips and incubated with different concentrations of CSE in serum-free DMEM medium for 48 h, then the medium was removed and cells were fixed with 4% formaldehyde in PBS solution at 4°C for 30 min. After three washes with PBS, the cells were stained with 10 mg/L Hoechst 33258 in PBS solution at room temperature in the dark for 1 h[16], and morphologic changes including cell shrinkage and nuclear condensation were observed under a fluorescence microscope (Olympus AX80, Olympus Corporation, Tokyo, Japan).

1.6.2 *Electron microscopy*

After CSE treatments, A549 cells were fixed in suspension ($\approx1\times10^6$ cells per specimen) with 3% glutaraldehyde in 0.1 mol/L PBS (pH 7.4) for 10 min at 4 °C and as a pellet for 2 h. After washed in the same buffer to which 0.2 mol/L sucrose had been added, the pellets were postfixed using 1% osmic acid in 0.1 mol/L sodium cacodylate (pH 7.3) for 30 min at room temperature, and then washed again in distilled water, stained *en bloc* with aqueous uranyl acetate, washed in distilled water, dehydrated in a graded series of ethanol, and embedded in Epon812 resin[17]. Ultra-thin sections were cut using an ultramicrotome, equipped with a diamond knife, and counterstained with lead citrate. They were examined under a JEM-1230 electron microscope (Japan Electron Optics Laboratory Co., Ltd. Mitaka, Tokyo, Japan) operating at 60 kV.

1.6.3 *Analysis of DNA fragmentation*

After 48 h of incubation with different concentrations of CSE, about 5×10^6 cells were harvested for every group by trypsinization and centrifuged at 1 000 r/min, and then incubated with 500 μl nuclear lysis solution (10 mmol/L Tris-HCl, pH 8.0, 150 mmol/L NaCl, 10 mmol/L EDTA, 0.4% SDS, 100 μg/ml proteinase K), 50 °C water bath for 3~5 h, 37 °C overnight, extracted using phenol (stabilized with 0.1mol/L Tris, pH 8.0), centrifuged at 6 000 r/min for 5 min. The acquired supernatant was extracted with 0.5 ml phenol/chloroform mixture (1:1), precipitated with 50 μl of 3 mmol/L sodium acetate and 2 ml of pre-cold alcohol, then centrifuged at 12 000 r/min for 10 min to precipitate DNA and air-dried. The DNA pellets were dissolved in 50 μl TE buffer and incubated with 5 μl RNase at 37 °C for 30 min respectively. A total of 20 μl samples were applied to a 1% agarose gel for electrophoresis at 50 V for 1.5 h. The gels were stained with ethidium bromide and visualized under ultraviolet transillumination[18].

1.6.4 *Annexin V binding experiment*

AnnexinV-FITC apoptosis detection kit was used to bind annexin V, which has a strong affinity for phosphatidylserine and can probe for apoptosis[19]. In brief, cells were harvested and washed twice with pre-chilled PBS (4 °C), and then resuspended in 250 μl binding buffer, at a final cell concentration of 1×10^6 cells/ml. Approximately 1×10^5 cells were incubated in the dark with 5 μl annexin V and 10 μl PI solution of 20 μg/ml for 15 min. Then the suspension was analyzed by using Coulter Epics XL flow cytometry. FITC and PI were excited at 488 nm, and the emission filters were 525 nm and 575 nm barrier filters respectively.

1.6.5 *Caspase-3 assay procedure*

Caspase-3 activity was detected by use of CaspGLOW™ fluorescein active caspase-3 staining kit. Briefly, cells were treated with different concentrations of CSE in culture flasks, concurrently a control culture was incubated without induction. After harvested, resuspended cells at a concentration of 1×10^6 cells/ml, removed 300 μl of aliquot from each of the induced and control cultures into Eppendorf tubes, added 1μl of FITC-DEVD-FMK into each tube and incubated for 30 min at 37 °C incubator with 5% CO_2. Centrifuged cells at 3 000 r/min for 5 min and removed supernatant, resuspended cells in 0.5 ml of wash buffer, and washed twice. For flow cytometric analysis, resuspended cells in 300 μl of wash buffer, kept samples on ice and analyzed samples by flow cytometry using the FL-1 channel.

1.6.6 *Fas expression*

After CSE treatment, cells were harvested with trypsin-

EDTA, washed three times with cold PBS, and resuspended in PBS to obtain a cell concentration of 1×10^6 cells/ml. For immunostaining with CD95, monoclonal antibody to human CD95 (Fas/APO-1)-FITC was used. Cells were incubated with FITC-conjugated Fas antibody (10 μg/ml) or with mouse IgG1 FITC (0.5 μg/ml) for 20 min in the dark and rinsed twice in PBS. Cells were resuspended in 1 ml of PBS and cell fluorescence intensities were measured using flow cytometry[11].

1.7 *Intracellular reactive oxygen species (ROS) measurement*

Intracellular ROS levels were measured with the use of fluorescent dye H_2DCFDA staining method[20]. H_2DCFDA is a nonpolar compound that is converted into a nonfluorescent polar derivative (H_2DCF) by cellular esterases after incorporated into cells. H_2DCF is membrane impermeable and rapidly oxidized to the highly fluorescent 2,7-dichlorofluorescein (DCF) in the presence of intracellular ROS[21]. Glass coverslips were coated with poly-*L*-lysine and placed in the wells of a 6-well culture plate. The cells were seeded into the wells at a density of 5.0×10^4 cells/well. After treatment, the cells were washed with prewarmed (37 °C) PBS once and then incubated for 30 min at 37 ºC with 20 μmol/L H_2DCFDA dissolved in PBS. Cover slips were then washed three times with PBS and analyzed under a TCS SP2 confocal laser microscope (Leica Corporate, Solms, Germany) with an excitation wavelength of 480 nm and an emission wavelength of 505~530 nm. The fluorescence intensity of staining was determined by densitometric scanning with LSM software (Leica Corporate, Solms, Germany).

1.8 *Statistical analysis*

All experiments were repeated twice or three times with duplicate samples each time. Results were presented as mean ± SD. Statistical analysis was performed using one-way ANOVA test and statistical significance is defined as $P<0.05$.

2 RESULTS

2.1 Effects of CSE on cell viability

CSE reduced cell viability in a time- and concentration-dependent manner (Fig.1). In the presence of 5% CSE, cell viability was reduced to 78.89% and 56.57% at 48 h and 72 h of incubation, respectively. After 48-hour or longer incubation, CSE at the concentrations of 10% or more reduced cell viability to 15.68%.

2.2 Cell cycle analysis

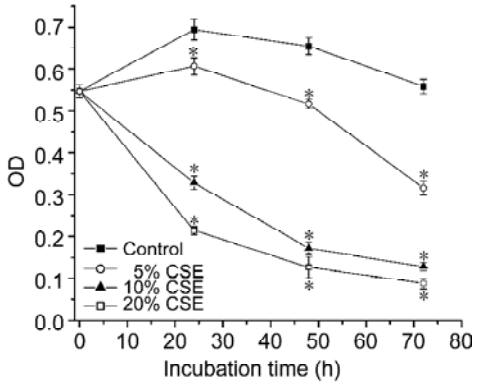

Fig.1. Time- and concentration-dependent effect of CSE on A549 cells. After incubation with 0, 5%, 10% and 20% CSE for 24 h, 48 h or 72 h, respectively, cell viability was evaluated by MTT assay. OD represents optical density of the MTT assay. $^*P<0.05$ *vs* control.

As shown in Table 1 and figure 2, after incubated with 5%, 10%, or 20% CSE for 48 h, the cells of G_1 phase were increased to (59.13 ± 0.95)%, (67.33 ± 0.91)% or (75.17 ± 1.31)%, respectively, and compared with control $P<0.01$, while cells in S and G_2/M phases were dramatically decreased. This indicated that the cell cycle was arrested in G_1 phase by CSE and the function was concentration-dependent.

Table 1. Percentage of cells in different phases of cell cycle after interfered with CSE at different concentrations (%)

Concentration of CSE	G_1	G_2	S
0 (control)	54.5 ± 0.60	8.83 ± 0.47	36.67 ± 1.00
5%	59.13 ± 0.95**	6.87 ± 0.32**	34.00 ± 1.06*
10%	67.33 ± 0.91**	3.77 ± 0.70**	28.90 ± 1.61**
20%	75.17 ± 1.31**	3.60 ± 0.36**	21.23 ± 1.66**
F	263.57	81.30	74.02
P	0.00	0.00	0.00

$^*P<0.05$, $^{**}P<0.01$ *vs* control. mean ± SD, $n=3$.

2.3 Morphological and DNA changes of A549 cells induced by CSE

2.3.1 Hoechst 33258 staining

After 48 h of incubation, 5% CSE induced chromatin condensation in ~23.5% of the cells, suggesting apoptotic cell death (Fig.3*B*). At the same time, ~35.2% of the cells incubated with 10% CSE were strongly stained with Hoechst 33258 (Fig.3*C*), however the cells with nuclei shrunken and chromatin condensation were reduced to 7.4% by induction of 20% CSE (Fig.3*D*).

2.3.2 Electron microscopy

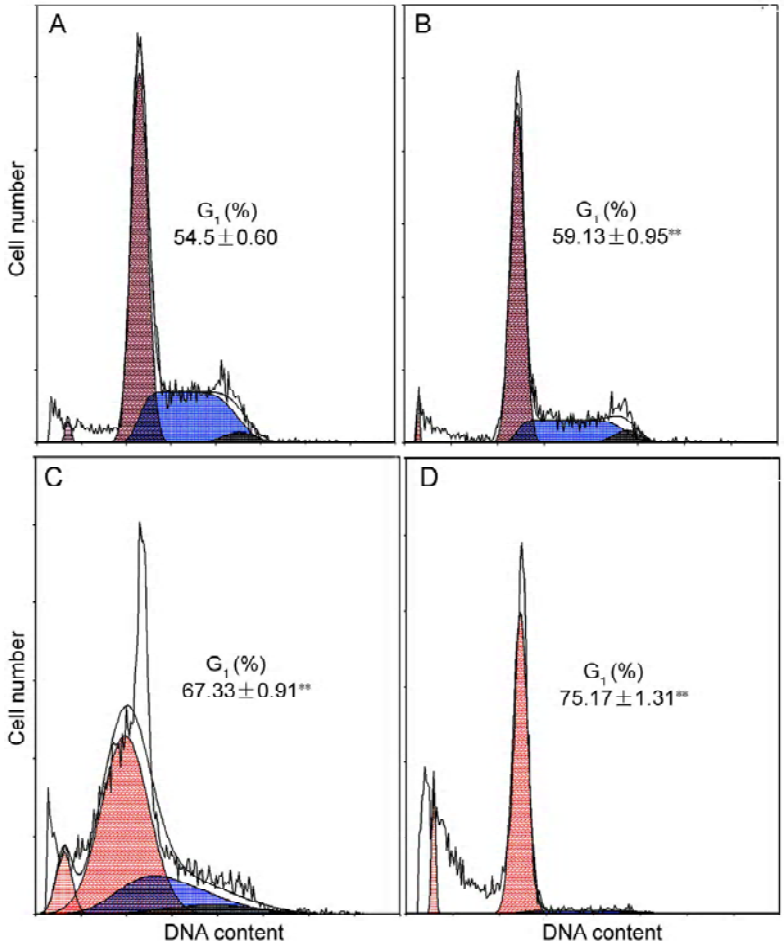

Fig.2. The results of DNA content analysis. After A549 cells were incubated with 0 (control, *A*), 5% (*B*), 10% (*C*) and 20% (*D*) CSE for 48 h, the cell percentage of G_1 phase in every group was analyzed by flow cytometry. The percentage of cells with diploid DNA is shown in each panel. Data from three independent experiments are presented as mean ± SD. $^{**}P<0.01$ *vs* control.

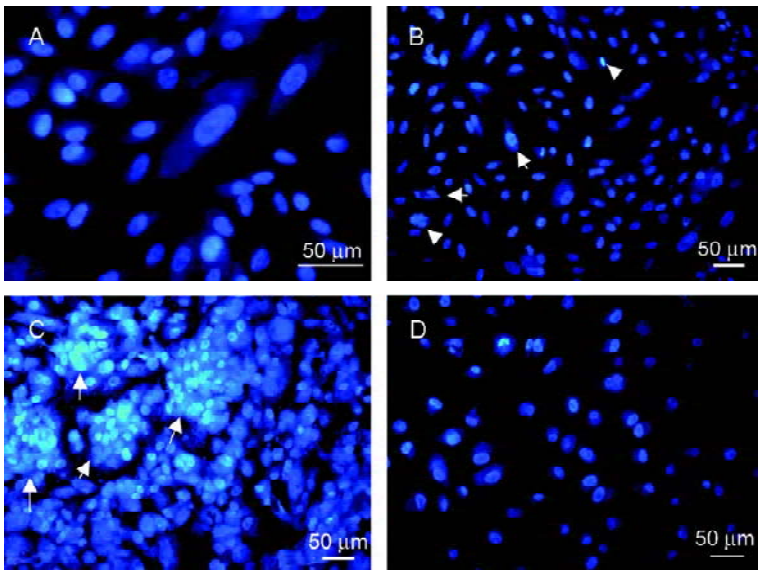

Fig.3. Morphological changes in A549 cells induced by CSE using Hoechst 33258 staining. After 48 h of incubation with culture medium, 5%, 10% or 20% CSE, respectively (*A*~*D*), the cells were stained with Hoechst 33258 and observed with fluorescence microscopy. Living cells have normal-shaped nuclei that are faintly stained with Hoechst 33258. Apoptotic cells have shrunken nuclei with chromatin condensation showed by arrows in the photos. Percentage of apoptotic cells was determined by counting at least 400 cells for each sample. Scale bar, 50 μm.

As displayed by electron micrographs, untreated cells showed integrated nuclear membrane, relatively homogeneous chromatin and extensive membrane interdigitations and microvilli (Fig.4*A*). After treated with 10% CSE for 48 h, A549 cells were characterized by condensation, margination of nuclear chromatin and many vacuoles in cytoplasm, at the same time, membrane microvilli were also disappeared (Fig.4*B*). All the changes indicated the apoptosis of A549 cells. Based on the above changes, the disruption and disappearance of nuclear membrane, even karyorrhexis were observed after incubation with 20% CSE, which were the characters of necrosis (Fig.4*C*).

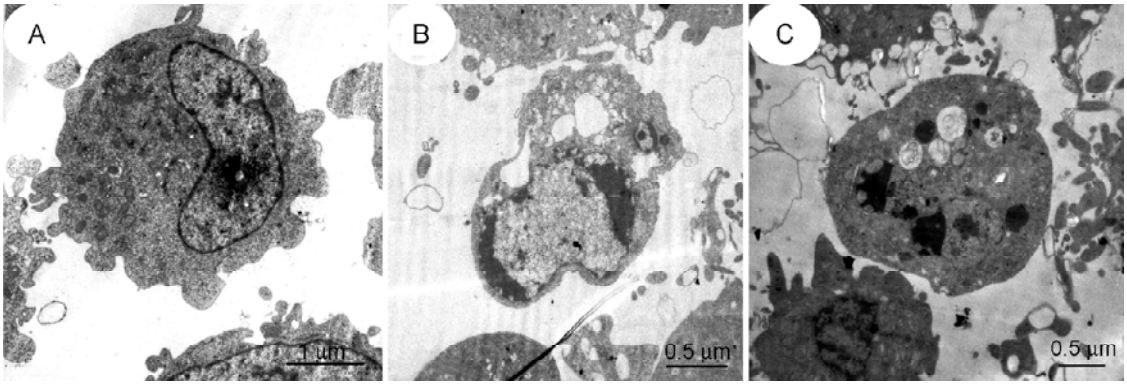

Fig.4. Electron micrographs of A549 cells stained with uranyl acetate and lead citrate. *A*: Control. Scale bar, 1 μm. *B*: Treated with 10% CSE for 48 h. A549 cells were characterized by condensation, margination of nuclear chromatin and many vacuoles in cytoplasm. Scale bar, 0.5 μm. *C*: Treated with 20% CSE for 48 h. A549 cells were characterized by the disappearance of nuclear membrane and karyorrhexis. Scale bar, 0.5 μm.

2.3.3 DNA fragmentation

Electrophoresis of the DNA fraction of the cells treated with CSE revealed a ladder formation of an ~200 bp fragment and its multiples (Fig.5), which also confirmed that incubation with 5% or 10% CSE induced apoptotic cell death.

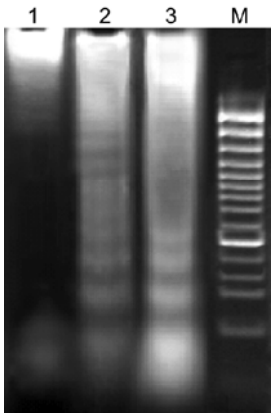

Fig. 5. Fragmentation of DNA in CSE-induced A549 cells. Lanes 1~3, DNA fractions of cells treated with culture medium, 5% or 10% CSE, respectively. M, DNA marker.

2.4 Annexin V-FITC staining

Apoptotic cells were detected using the calcium-binding protein annexin V. In particular, phosphatidylserine residues, which are normally located in the internal phospholipid layer, are actively translocated to the external layer in apoptotic cells and thus become detectable by annexin V. Because only using annexin V staining can't distinguish between apoptotic and necrotic cells, we used PI to identify necrotic cells. As shown in Fig.6, after treated with 5% and 10% CSE, apoptotic cells were greatly increased to 28.6% and 41.2% compared with only 2.54% in the control group, which demonstrated that CSE could induce apoptosis of alveolar epithelial cells in a certain dose. When the concentration of CSE increased to 20%, the proportion of apoptotic cells decreased to 3.28%, but the necrotic cells dramatically increased to 35.1% compared with 8.03% and 5.72% in those groups incubated with 5% and 10% CSE, respectively. This indicated high concentration of CSE mainly caused necrosis instead of apoptosis.

2.5 The expressions of activated caspase-3 and Fas receptor after CSE treatment

After treatment with CSE for 24 h, A549 cells with activated caspase-3 were increased from only (9.33 ± 0.61)% in the control group to (65.2 ± 1.42)% and (91.5 ± 1.16)% in 5% or 10% CSE groups, the corresponding mean fluorescence intensities simultaneously increased to (12.4 ± 0.85) and (41.6 ± 1.11) compared with (5.03 ± 0.29) in untreated cells (Table 2 and Fig.7).

After incubated with CSE for 48 h, A549 cells expressing Fas significantly increased to (43.3 ± 1.07)% and (86.0± 0.61)% after treated with 5% or 10% CSE compared with (6.54 ± 0.90)% in the control group. At the same time, their mean fluorescence intensities were also greatly changed

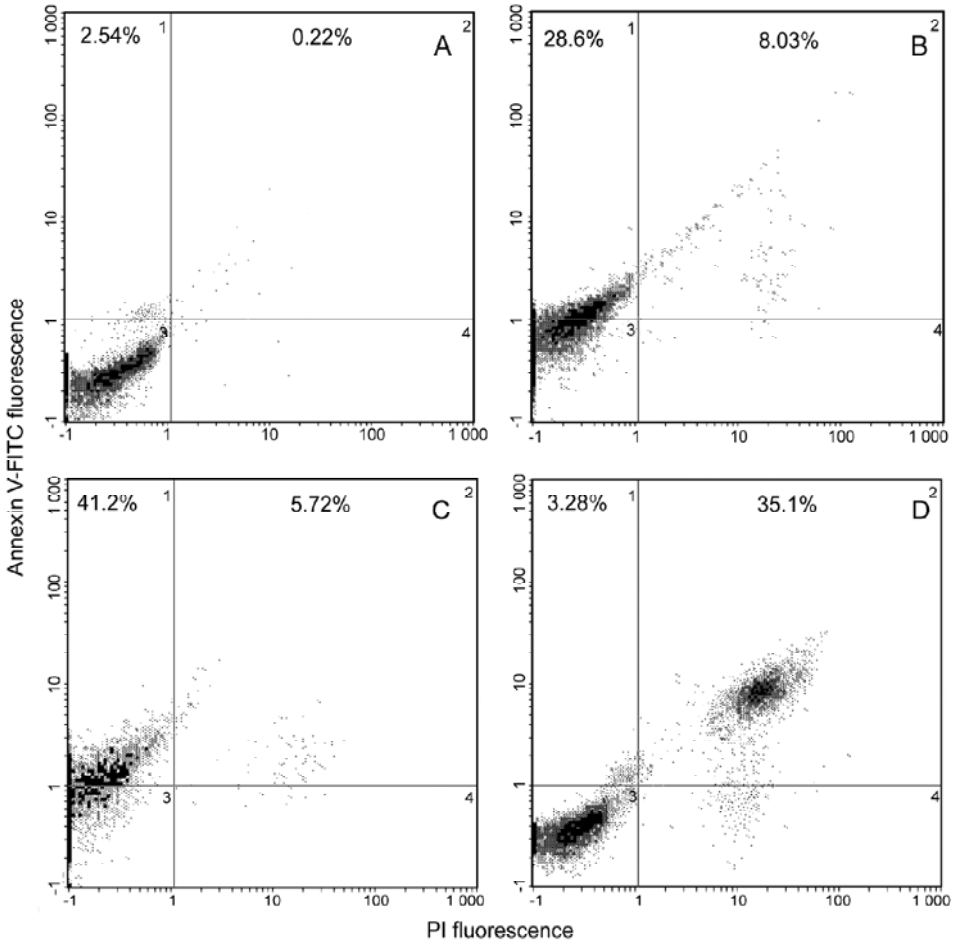

Fig. 6. The results obtained using annexin V-FITC/PI staining. A549 cells were treated with culture medium (*A*), 5% (*B*), 10% (*C*) and 20% (*D*) CSE for 16 h respectively, and then double stained with annexin V-FITC and PI followed by flow cytometric analysis. 10 000 cells were detected for every samples. Living cells are in the bottom left quadrants, apoptotic cells in the upper left quadrants, and necrotic or late apoptotic cells in the upper right quadrants. Cell percentage related with apoptosis or necrosis was presented in their corresponding quadrants.

Table 2. The positive rate of A549 cells with activated caspase-3 and Fas and the corresponding mean fluorescence intensities after treatment with CSE for 24 h or 48 h respectively

Concentration of CSE	Positive rate (%)		Mean fluorescence intensity	
	Activated caspase-3	Fas	Activated caspase-3	Fas
0 (control)	9.33 ± 0.61	6.54 ± 0.90	5.03 ± 0.29	1.72 ± 0.10
5%	65.2 ± 1.42*	43.3 ± 1.07*	12.4 ± 0.85*	7.85 ± 0.36*
10%	91.5 ± 1.16▼	86.0 ± 0.61▼	41.6 ± 1.11▼	29.3 ± 0.93▼

*P<0.01 *vs* control, ▼P <0.01 *vs* 5% CSE group. mean ± SD, n=3.

from (1.72 ± 0.10) in the control group to (7.85 ± 0.36) and (29.3 ± 0.93) in 5% or 10% CSE group respectively (Table 2 and Fig.8).

2.6 The level of intracellular ROS

After incubation with CSE from 5% to 20% for 3 h, intracellular ROS levels were detected by laser confocal microscopy, and the results were expressed as arbitrary fluorescence units. Compared with control, intracellular ROS levels were dramatically increased in CSE-treated groups, and it was concentration-dependent (Fig.9).

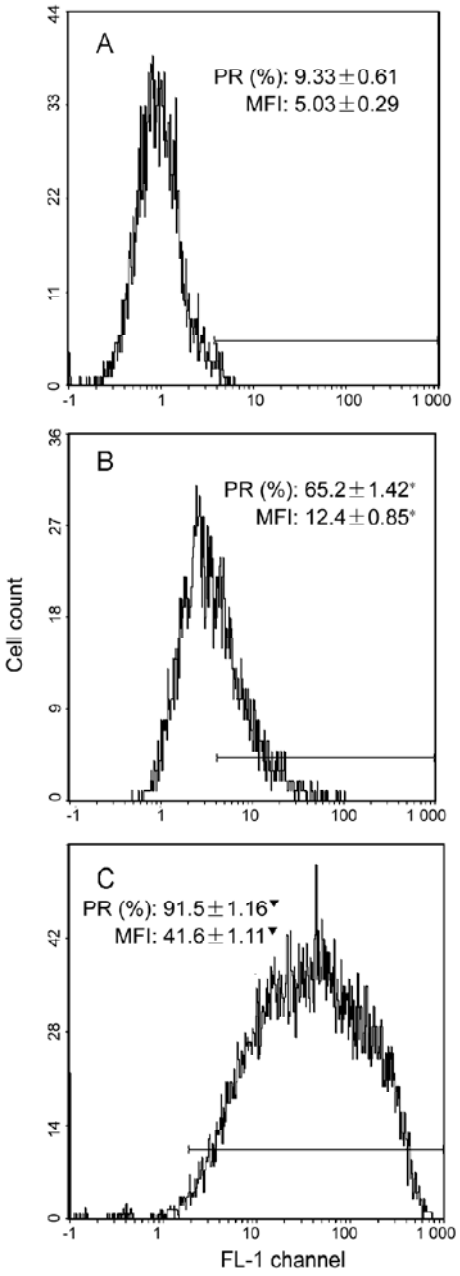

Fig.7. Expression of activated caspase-3. After A549 cells were treated with culture medium (*A*), 5% (*B*) or 10% (*C*) CSE for 24 h, activated caspase-3 was detected using its inhibitor DEVD-FMK conjugated to FITC and analyzed by flow cytometry. PR is abbreviation for positive rate, and MFI is for mean fluorescence intensity. *$P<0.01$ *vs* control, ▼$P<0.01$ *vs* 5% CSE group. This is a representative of three independent experiments.

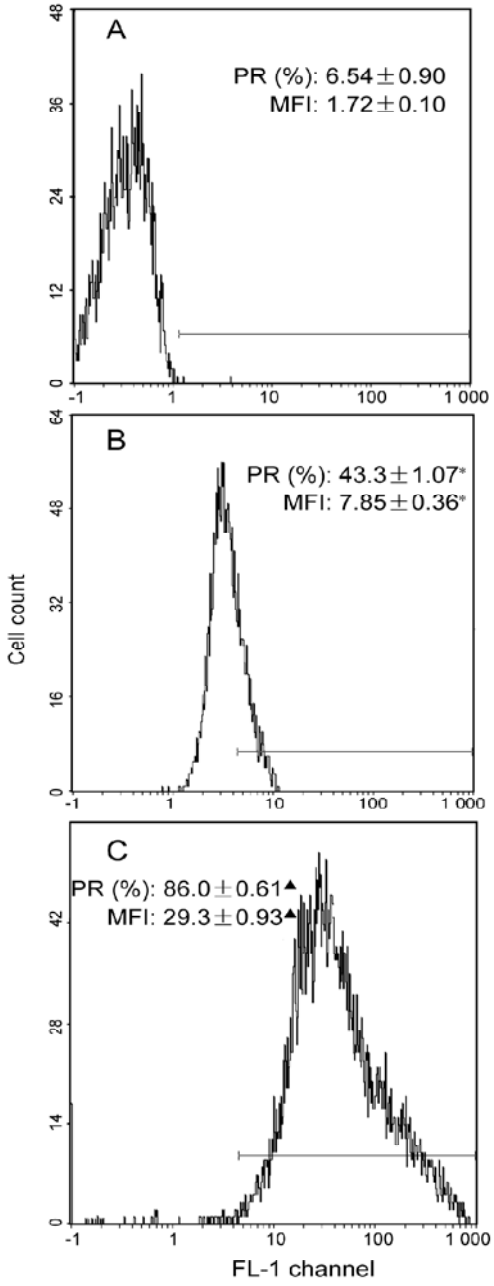

Fig.8. Fas receptor expression after CSE treatment. After A549 cells were treated with culture medium (*A*), 5% (*B*) or 10% (*C*) CSE for 48 h, Fas expression was detected by immunostaining with FITC conjugated Fas antibody and analyzed by flow cytometry. PR is abbreviation for positive rate, and MFI is for mean fluorescence intensity. *$P<0.01$ *vs* control, ▲$P<0.01$ *vs* 5% CSE group. This is a representative of three independent experiments.

3 DISCUSSION

In the present study, CSE exposure resulted in a time- and dose-dependent loss of cell viability in A549 cells as detected using MTT assay. According to the results of flow cytometric analysis, for the first time it was documented that cell cycle stage of alveolar epithelial cells induced by CSE was arrested in G_1 phase. At low CSE concentrations

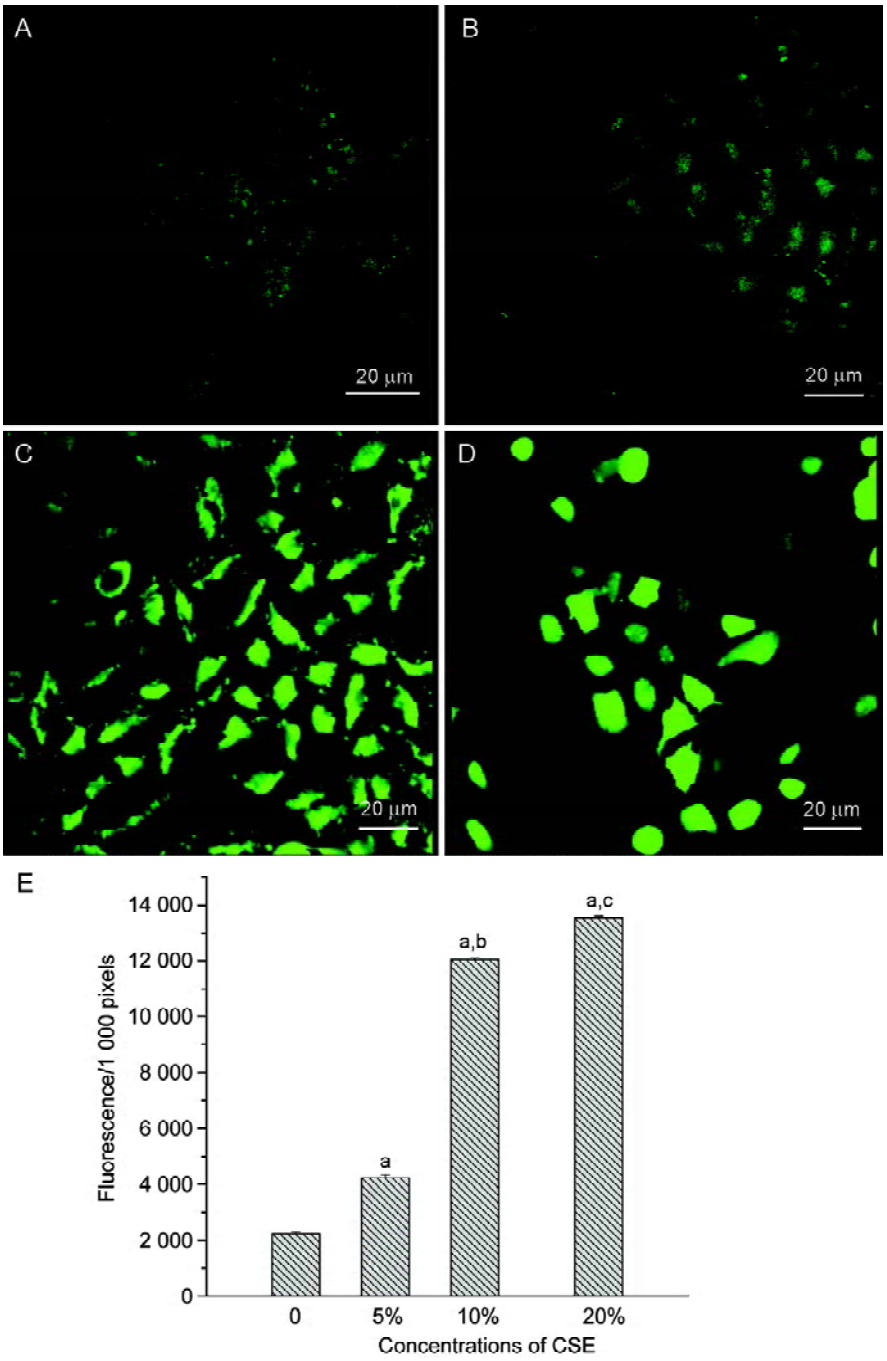

Fig.9. The levels of ROS in A549 cells after incubation with CSE. After treatment with culture medium (*A*), 5% (*B*), 10% (*C*) or 20% (*D*) CSE for 3 h, the ROS levels in A549 cells were examined using laser confocal microscopy. Scale bar, 20 μm. *E*: Quantitative representation of ROS levels. Data were obtained from fluorescence intensity analysis of interested areas in acquired photos using Leica Confocal Software and presented as means±SD for four samples from three separate experiments, and the results were expressed in arbitrary fluorescence units of 1 000 pixels. $^{a}P<0.01$ *vs* control, $^{b}P<0.01$ *vs* 5% CSE group, $^{c}P<0.01$ *vs* 10% CSE group.

within 10%, apoptotic cell death was induced, and at higher doses, necrosis occurred. These were confirmed by classic DNA laddering of fragmented DNA as well as ultrastructural analysis and Hoechst staining showing several morphological alterations related with apoptosis such as chromatin condensation, nuclear indentations, cytoplasmic mass decrease, and overall cell shrinkage. When treated with 20% CSE, A549 cells were characterized by the dis-

appearance of nuclear membrane and karyorrhexis which are characters of necrosis. In the experiment, the externalizaion of phosphatidylserine residue was increased greatly by 5% and 10% CSE treatment as detected by annexin V-FITC staining. To distinguish apoptosis from necrosis, PI was used to stain nuclei. It was demonstrated higher proportion of necrotic cells produced by 20% CSE. The results further confirmed the effects of CSE on A549 cells in morphology and cell cycle progression. Besides, our findings in the study indicated the involvement of caspase-3, which is a major executioner of apoptosis, in the process of CSE treatment.

Interestingly, the result from lower concentrations of CSE was contrary to what Wickenden *et al*.[10] offered previously. To pursue the cause of the discrepancy, we compared the concentrations of CSE used in the two studies. In the work of Wickenden *et al*., CSE was prepared freshly at a concentration of 1 cigarette/ml in CMF-PBS; while we used two cigarettes bubbled through 50 ml of serum-free DMEM. On the assumption that the efficiency in preparing CSE in the two experiments was the same, the concentration of CSE in their experiment was almost 25-fold higher than what we used in the present study. This may partly explain the opposite results in the experiment because we also observed the occurrence of dramatic necrosis when concentration of CSE was increased to 20%, which was quite close to the dose of 1% CSE, the lowest concentration of CSE used in the study of Wickenden *et al*.[10]. It could be speculated that high concentration of CSE was the reason that necrosis instead of apoptosis was observed in their study. CSE could be prevented by the presence of extracellular thiol compounds such as GSH, which is native to the lung and forms one of the most important lung antioxidant defenses[22]. Therefore, it could be deduced that the risk of necrosis in response to cigarette smoking is insignificant. In the study *in vitro*, after oxidant injury, neither extracellular nor intracellular antioxidants can be enough supplemented in time as *in vivo*, considering the relatively weak antioxidant defense, a lower concentration of CSE may more virtually mimic the process of interaction between CSE and alveolar epithelial cells *in vivo*. Although no standardized protocol for the production of CSE exists, each procedure can isolate a slightly different spectrum of components. Nevertheless, we believe that our method of exposing cells to CSE more accurately mimics smoke filling the airspace and exposing to the lung lining fluid.

For the first time, our results indicated death receptor pathway involving Fas might exist in CSE-induced apoptosis of alveolar epithelial cells. Cigarette smoking is a major cause of human lung injury, although the pathogenic mechanism remains unknown. Increasing evidence suggests that high concentrations of ROS are involved in many of chronic diseases associated with smoking. Fas tyrosine phosphorylation is suggested to be the way in which cigarette smoking triggers apoptosis. In addition, it is generally accepted that protein tyrosine kinase activation is an early signal in Fas-induced apoptosis because Fas/FasL ligation rapidly induces the tyrosine phosphorylation of multiple cellular proteins. Once induced, the FasL contributes to cell death by activating its receptor Fas, which in turn leads to tyrosine phosphorylation of Fas, activation of caspase cascade and cell death. In addition, the studies of Kuo *et al*.[23] implicate the p38/c-Jun N-terminal kinase (JNK) > Jun > FasL > Fas signaling cascade in cigarette smoking mediated death of rat lung tissue. In the present study, rapid and accelerating induction of intracellular ROS was documented along with the gradient increase of CSE, which is demonstrating that CSE-induced apoptosis of alveolar epithelial cells may be via ROS generation, which in turn may lead to the phosphorylation of p38/JNK mitogen-activated protein kinases family (MAPK) pathway and then activation of Fas cascades. This effect may be an important pathway in the pathogenesis of emphysema induced by CSE.

From the present experiment we conclude that cell cycle stage of alveolar epithelial cells induced by CSE is arrested in G_1 phase; CSE induces apoptosis of alveolar epithelial cells involving activation of caspase-3 at lower concentrations; Fas receptor is involved in CSE-induced apoptosis of human alveolar epithelial cells; CSE-induced accumulation of intracellular ROS may be an initiator of the apoptotic or necrotic cell death of alveolar epithelial cells.

Although we found some proofs of CSE-induced apoptosis in alveolar epithelial cells, further experiments are still necessary to reveal other possible apoptotic pathways such as mitochondria pathway and so on. The CSE used in the study were prepared by an *in vitro* system that bypassed important biological interactions. Therefore, it is urgent to construct validated *in vivo* models in order to elucidate the exact mechanisms of COPD involving CSE.

REFERENCES

1 Pryor WA, Stone K. Oxidants in cigarette smoke. Radicals, hydrogen peroxides, peroxynitrate, and peroxynitrite. Ann NY Acad Sci 1993; 686: 12-28.

2 Rahman I, MacNee W. Lung glutathione and oxidative stress: implications in cigarette smoke-induced airways disease. Am J

Physiol 1999; 277: L1067-L1088.

3 Riley DJ, Kerr JS. Oxidant injury of the extracellular matrix: potential role in the pathogenesis of pulmonary emphysema. Lung 1985; 163:1-13.

4 Gadek JE, Pacht ER. The protease-antiprotease balance within the human lung: implications for the pathogenesis of emphysema. Lung 1990; 168:552-564.

5 Tuder RM, Wood K, Taraseviciene L, Flores SC, Voekel NF. Cigarette smoke extract decreases the expression of vascular endothelial growth factor by cultured cells and triggers apoptosis of pulmonary endothelial cells. Chest 2000; 117: 241S-242S.

6 Yuma H, Tadashi M, Sonoko N, Hiroyuki M, Isao I, Takateru I. Cytotoxic effects of cigarette smoke extract on an alveolar type II cell-derived cell line. Am J Physiol Lung Cell Mol Physiol 2001; 281: L509-L516.

7 Kasahara Y, Tuder RM, Taraseviciene-Stewart L, Le Cras TD, Abman S, Hirth PK, Waltenberger J, Voelkel NF. Inhibition of VEGF receptors causes lung cell apoptosis and emphysema. J Clin Invest 2000; 106: 1311-1319.

8 Lucey EC, Keane J, Kuang PP, Snider GL, Goldstein RH. Severity of elastase-induced emphysema is decreased in tumor necrosis factor-alpha and interleukin-1beta receptor-deficient mice. Lab Invest 2002; 82:79-85.

9 Yasunori K, Rubin MT, Carlyne DC, David AL, Sonia CF, Norbert FV. Endothelial cell death and decreased expression of vascular endothelial growth factor and vascular endothelial growth factor receptor 2 in emphysema. Am J Respir Crit Care Med 2001; 163: 737-744.

10 Wickenden JA, Clarke MC, Rossi AG, Rahman I, Faux SP, Donaldson K, MacNee W. Cigarette smoke prevents apoptosis through inhibition of caspase activation and induces necrosis. Am J Respir Cell Mol Biol 2003; 29(5): 562-570.

11 Besnard V, Corroyer S, Trugnan G, Chadelat K, Nabeyrat E, Cazals V, Clement A. Distinct patterns of insulin-like growth factor binding protein (IGFBP)-2 and IGFBP-3 expression in oxidant exposed lung epithelial cells. Biochim Biophys Acta 2001; 1538: 47-58.

12 Fine A, Anderson NL, Rothstein TL, Williams MC, Gochuico BR. Fas expression in pulmonary alveolar type II cells. Am J Physiol 1997; 273: L64-L71.

13 Harvey C, Aaron J. Possible mechanisms of emphysema in smokers. *In vitro* suppression of serum elastase-inhibitory capacity by fresh cigarette smoke and its prevention by antioxidants. Am Rev Respir Dis 1978; 118: 617-621.

14 Dariusz S, Sarah JS, Richard HC, Michael B. An improved MTT assay. J Immunol Methods 1993; 157: 203-207.

15 Kim H, Liu X, Kobayashi T, Conner H, Kohyama T, Wen FQ, Fang Q, Abe S, Bitterman P, Rennard SI. Reversible cigarette smoke extract-induced DNA damage in human lung fibroblasts. Am J Respir Cell Mol Biol 2004; 31: 483-490.

16 Li HL, Ye KH, Zhang HW, Luo YR, Ren XD, Xiong AH, Situ R. Effect of heparin on apoptosis in human nasopharyngeal carcinoma CNE2 cells. Cell Res 2001; 11(4): 311-315.

17 Polla BS, Kantengwa S, Francois D, Salvioli S, Franceschi C, Marsac C, Cossarizza A. Mitochondria are selective targets for the protective effects of heat shock against oxidative injury. Proc Natl Acad Sci USA 1996; 93: 6458-6463.

18 Wang J, Wilcken DE, Wang XL. Cigarette smoke activates caspase-3 to induce apoptosis of human umbilical venous endothelial cells. Mol Genet Metab 2001; 72: 82-88.

19 Liu XM, Chapman GB, Wang H, Durante W. Adenovirus-mediated heme oxygenase-1 gene expression stimulates apoptosis in vascular smooth muscle cells. Circulation 2002; 105: 79-84.

20 Chan WH, Wu HJ, Hsuuw YD. Curcumin inhibits ROS formation and apoptosis in methylglyoxal-treated human hepatoma G_2 cells. Ann NY Acad Sci 2005; 1042: 372-378.

21 Sauer H, Klimm B, Hescheler J, Wartenberg M. Activation of p90RSK and growth stimulation of multicellular tumor spheroids are dependent on reactive oxygen species generated after purinergic receptor stimulation by ATP. FASEB J 2001; 15: 2539-2541.

22 Kelly FJ. Gluthathione: in defence of the lung. Food Chem Toxicol 1999; 37: 963-966.

23 Kuo WH, Chen JH, Lin HH, Chen BC, Hsu JD, Wang CJ. Induction of apoptosis in the lung tissue from rats exposed to cigarette smoke involves p38/JNK MAPK pathway. Chem Biol Interact 2005; 155: 31-42.